Microbial evolution reshapes soil carbon feedbacks to climate change

Elsa Abs[1,2*], Scott R. Saleska[1], Regis Ferriere[1,2,3]

[1] Department of Ecology & Evolutionary Biology, University of Arizona, Tucson, AZ 85721, USA

[2] Institut de Biologie de l'Ecole Normale Supérieure (IBENS), ENS-PSL University, CNRS, INSERM, 75005 Paris, France

[3] International Center for Interdisciplinary Global Environmental Studies (iGLOBES), CNRS, ENS-PSL University, University of Arizona, Tucson, AZ 85721, USA

*Corresponding author, abs@biologie.ens.fr

Abstract

Microbial decomposition of soil organic matter is a key component of the global carbon cycle. As Earth's climate changes, the response of microbes and microbial enzymes to rising temperatures will, though emission of additional CO2, largely determine the soil carbon feedback to climate. However, while increasing attention focuses on physiological and ecological mechanisms of microbial responses, the role of evolutionary adaptation to warming has been little studied. To address this gap, we developed an eco-evolutionary model of a soil microbe-enzyme system under warming. Constraining the model with observations from five contrasting biomes reveals that evolution will likely aggravate soil carbon losses to the atmosphere, a positive feedback to climate change. The model reveals a strong latitudinal gradient in evolutionary effects, driven mostly by initial temperature, from small evolutionary effects at low (warm) latitudes to large effects at high (cold) latitudes. Accounting for evolutionary mechanisms will likely be critical for improving projections of Earth system responses to climate change.

Introduction

Microorganisms are key drivers of global biogeochemical cycles[1]. In terrestrial ecosystems, soil microbes decompose organic matter, returning carbon to the atmosphere as carbon dioxide (CO_2)[2]. *In vitro* and *in situ* experiments suggest that changes in microbial decomposition with warming are an important feedback to climate[3–5]. Soil microbial populations may respond to increasing temperature through physiological mechanisms such as individual metabolic adjustment[6,7] and ecological mechanisms such as shifts in population abundance or community composition[8,9]. Given the short generation time, large population sizes and standing genetic variation of many microbial organisms, evolutionary adaptive responses of microbial populations to warming are also likely[10,11]. However, how microbial evolutionary adaptation may contribute to carbon-climate feedbacks is unknown[12].

Key to microbial decomposition of soil organic matter is the production by microbes of extracellular enzymes (exoenzymes), that diffuse locally in the soil and bind to soil organic matter compounds[13]. Because the fitness cost of exoenzyme production[14] (reduced allocation to growth, Fig. 1a) is paid by individual microbes whereas fitness benefits (larger resource pool) are enjoyed by microbial collectives[15], we expect genetic variation in exoenzyme production[16] to be under strong selection[15,17]. Our objective is to evaluate how exoenzyme production responds to selection under environmental warming, and how the evolutionary response of exoenzyme production impacts the response of soil organic carbon stock (SOC). To this end, we develop and analyze a novel eco-evolutionary model, modified from that of ref. 18[18] (Fig. 1a), to take microbial evolutionary adaptation into account.

In this novel eco-evolutionary model, the focal microbial adaptive trait is the fraction of assimilated carbon allocated to exoenzyme production[19,20], or 'exoenzyme allocation fraction', hereafter denoted by φ. The balance of assimilated carbon, $1-\varphi$, is allocated to microbial growth. Allocated carbon is then converted to exoenzymes or microbial biomass with, respectively, enzyme production efficiency γ_Z and microbial growth efficiency γ_M,

while the balance is respired and lost as CO2 in order to produce the metabolic energy needed for enzyme or biomass production (see Fig. 1a and Methods). Competition between microbial strains differing in enzyme allocation fraction φ drives adaptive evolution. The model predicts the adapted value, φ^*, of the exoenzyme allocation fraction at any given temperature; the adaptive response of the exoenzyme allocation fraction to temperature rise; and how this response impacts the decomposition rate and SOC stock. By comparing the full eco-evolutionary (ECOEVO) response of SOC stock to the purely ecological (ECO) response in absence of evolution (in which φ is a fixed parameter that does not change), we can evaluate the contribution of microbial evolutionary adaptation (EVO effect) to the direction and magnitude of the SOC stock response to climate warming (Fig. 1b, c).

Results

Scenarios of microbial temperature dependence. Microbial decomposition is predicted to respond to warming due to the temperature sensitivity of intra- and extra-cellular enzymatic activity[21–23]. In our baseline 'kinetics-only' scenario of temperature-dependent decomposition, we assume that microbial uptake parameters (maximum uptake rate and half-saturation constant) and exoenzyme kinetics parameters (maximum decomposition rate and half-saturation constant) increase with temperature[5,24]. We consider two additional scenarios for the influence of temperature on decomposition. In the microbial mortality scenario, the microbial death rate also increases with temperature[25]. This could be due to a higher risk of predation or pathogenic infection at higher temperatures, or faster microbial senescence due to higher protein turnover[25]. In the microbial growth efficiency (MGE) scenario, MGE (the fraction of carbon allocated to growth that actually contributes to microbial biomass, as opposed to being released as CO_2 via growth respiration) decreases with temperature[18,26], which could be due to higher maintenance costs at higher temperature[27].

Evolution of the enzyme allocation fraction trait. At any given temperature, the evolutionary model predicts that the adapted value of the enzyme allocation fraction, φ^*, depends on four parameters (equation (5) in Methods): MGE, mortality, maximum uptake rate, and local competitive advantage to exoenzyme producers, or 'competition asymmetry'. Among these parameters, competition asymmetry quantifies the accessibility of the exoenzyme 'public good' to microbes. It measures the differential availability of enzymatically produced dissolved organic carbon (DOC) to different microbial strains. Competition asymmetry is shaped by diffusion of exoenzymes and DOC, and by microbial mobility, and is thus likely influenced by soil physical properties, such as texture or moisture. For simplicity, we assume that competition asymmetry is independent of temperature.

Comparing ECO and ECOEVO responses of soil carbon to warming. In all three scenarios of temperature dependence, the pure ecological (not including evolution) equilibrium of SOC generally decreases as temperature or exoenzyme allocation fraction increases (Fig. 1b, Supplementary Fig. 4, Supplementary Note 5). This evolution-independent (ECO) response results in the lost carbon being released to the atmosphere as CO2, a positive feedback to warming consistent with previous models.

With the eco-evolutionary (ECOEVO) version of the model, and focusing on the baseline scenario of temperature dependence, we find that evolution causes the adapted enzyme allocation fraction, φ^* (which is held constant in the pure ECO model runs), to always increases with increasing temperature (Fig. 1b, Supplementary Fig. 5a). Combining both results, we conclude that the ECOEVO response mediated by microbial evolution amplifies the ecology-driven loss of soil carbon due to warming (ECO response) (Fig. 1c).

The effect of evolution (EVO effect) is strong when the ECOEVO response markedly departs from the ECO response. This is predicted in cold ecosystems harboring communities of slow-growing microbes, under soil conditions that give only a small competitive edge to greater enzyme producers (Fig. 2, Supplementary Fig. 6). Strong EVO

effects are robust to the other model parameters – enzyme parameters (efficiency, production) and environmental parameters (litter input, leaching) (Supplementary Figs. 6 and 7, Supplementary Note 4).

We address the robustness of strong evolutionary effects (Fig. 3a) to different scenarios of temperature dependence by focusing on values of nutrient uptake parameters, litter input, and competition asymmetry that are conducive to such large EVO effects (for example, point B2 in Fig. 2b). In the temperature-dependent mortality scenario, how the direction and magnitude of the EVO effect changes from the baseline scenario is entirely determined by the sensitivity of microbial mortality to warming. When mortality is moderately sensitive to temperature, the ECO and ECOEVO responses become more similar, resulting in a smaller EVO effect (Fig. 3a, b). When mortality is strongly sensitive to temperature, the ECOEVO response becomes weaker than the ECO response, which implies that evolution buffers the loss of soil carbon (negative EVO effect, Fig. 3c). Such EVO effects are predicted to be stronger in *warmer* ecosystems (higher T_0, Fig. 3c; see also Supplementary Note 7).

In the temperature-dependent MGE scenario, the direction and magnitude of the ECOEVO response to warming vary dramatically with the initial temperature T_0 (Fig. 3d). Driven by adaptive evolution, the enzyme allocation fraction increases strongly with warming in cold systems, hardly changes in temperate systems, and decreases markedly in warm systems (Supplementary Fig. 5d), with parallel effects on the decomposition rate (Supplementary Fig. 5h). As a consequence, at low T_0, aggravation of soil carbon loss by evolution is almost as severe as in the baseline scenario, even though both ECO and ECOEVO responses are weaker in this scenario (Fig. 3a, d). At higher values of T_0, the ECOEVO response becomes weaker than the ECO response or even positive (Fig. 3d), resulting in the sequestration rather than loss of soil carbon.

Model predictions using empirical data from five biomes. To illustrate how EVO effects may vary in real ecosystems, we used available data[22] on the decomposition kinetic

parameters in five biomes of increasing latitude and decreasing mean annual temperature (Costa Rica, California, West Virginia, Maine, and Alaska, Fig. 4). We evaluated ECO and ECOEVO responses for each biome under three levels of competition asymmetry (as quantified by the local competitive advantage to producers, c_0) (Fig. 4a-h). Under our baseline scenario, EVO effects correlate strongly with mean annual temperature, even more so for low competition asymmetry (Fig. 4i). Stronger EVO effects occur in colder biomes, as found in the general analysis (Fig. 3a). In contrast, the ECO response does not correlate with mean annual temperature (Fig. 4a). As a result, a temperate biome such as Maine exhibits a weak ECO response that can be strongly amplified by evolution, whereas the warm Costa Rica biome shows a strong ECO response that is little affected by evolution.

These results are quantitatively attenuated but qualitatively unaffected when microbial mortality increases moderately with temperature (Fig. 4b, f, j). With a stronger effect of temperature on microbial mortality, all biomes show the evolutionary buffering effect (Fig. 4k) found in the general analysis (Fig. 3c). The intensity of evolutionary buffering is independent of the biomes' mean annual temperature, whereas it varies significantly with competition asymmetry (Fig. 4k). Under the temperature-dependent MGE scenario, ECO and ECOEVO responses are reduced in magnitude compared to the baseline scenario (Fig. 4d, h), particularly in cold biomes. However, in these biomes, EVO effects are enhanced dramatically (Fig. 4l). Thus, in a biome as cold as Alaska, a significant ECOEVO loss of soil carbon is predicted, whereas the purely ecology-driven loss of soil carbon would be negligible (Fig. 4l).

Discussion

As global warming increases environmental temperatures, our model predicts evolution of the enzyme allocation fraction, with potentially large effects on the decomposition process and SOC stock. The size of evolutionary (EVO) effects is most sensitive to MGE, microbial mortality, activation energy of uptake maximal rate, competition asymmetry, and initial temperature (Fig. 2). Evolution often aggravates the ecological loss of soil carbon in

response to warming, especially in cold biomes (Figs. 1, 3). We identified two cases in which evolutionary adaptation to warming may buffer or even revert the ecology-driven loss of soil carbon: strongly temperature-dependent microbial mortality, or temperature-dependent MGE in warm ecosystems (Fig. 3). Overall, we expect evolutionary effects to vary greatly among ecosystems that differ in biotic (microbial life history and physiology) and abiotic (temperature, soil texture and moisture) characteristics.

Implications of our findings for large geographic scales, across terrestrial ecosystems, are hinted at by specifying the model for the five contrasting biomes for which exoenzyme kinetics data are available[22]. We find evolutionary aggravation of soil carbon loss to be the most likely outcome, with a strong latitudinal pattern induced by temperature, from small evolutionary effects at low (warm) latitudes to large evolutionary effects at high (cold) latitudes. In all cases, competition asymmetry is a strong influence on the eco-evolutionary response of microbial decomposition to warming (Fig. 4). Soil texture and moisture, which may influence competition asymmetry, vary considerably among locations[22]. Predicting geographic variation in ECOEVO responses and EVO effects across large geographic scales thus calls for more empirical data on variation in ecological (competition) traits, especially how the competitive advantage to exoenzyme producers varies with soil physical properties.

Large-scale projections of soil C cycle changes on timescales that are long relative to the characteristic times of the processes described by our model also raise the issue of distinguishing between readily available SOM versus physio-chemically protected SOM, which decomposes more slowly[5,28]. Reinterpreting the soil carbon stock compartment of our model as readily available SOM removes the constraint of having the stock of microbial biomass, M, much smaller than SOC (C in our model)[29,30]. The relevant measure of soil carbon then becomes the sum of all compartments, $C_{tot} = C + M + Z + D$, called 'total soil active carbon', where Z is the exoenzyme concentration and D the biomass of dissolved organic carbon (equations (1a-d) in online Methods). We investigated how our results are changed when ECO and ECOEVO responses are defined with respect to C_{tot}, rather than C,

focusing on the baseline scenario (constant MGE and constant microbial turnover). Supplementary Figure 9 exemplifies the case where microbial biomass is the main component of C_{tot} and total soil active carbon is higher in the presence of microbes than in their absence. This occurs because here a higher SOC leaching rate, e_C, is more than compensated by the microbial higher productivity (high MGE, γ_M, and low death rate, d_M), so that carbon is retained in the soil longer in the presence of microbes than without. In this type of high-leaching soils, the direction of the ECO response shifts from negative (carbon loss) to positive (carbon gain). Microbial adaptive evolution can amplify, buffer or reverse this ecological response depending on the local competitive superiority of enzyme producers, c_0 (Supplementary Fig. 10). This is because microbial biomass, M, is the main carbon stock in these systems and purely ecological processes drive an approximately linear increase in M with temperature whereas M responds non-linearly to the increase in enzyme allocation fraction (Supplementary Fig. 9b).

Our study demonstrates how a trait-based approach can be used to integrate microbial evolutionary adaptation into carbon cycle models[31]. Our focal trait, the enzyme allocation fraction, φ, is pivotal in the decomposition process. Other microbial traits that appear in our model may also respond to selection imposed by warming, such as MGE (γ_M) and the exoenzyme production efficiency (γ_Z). The γ_M trait may evolve in response to variation in environmental quality (e.g. predation or infection risk), possibly trading-off with the maximum rate of uptake or correlating with the death rate; γ_Z may evolve in response to substrate variation[20], possibly correlating with the enzyme decay rate. Given specific assumptions about factors of and constraints on the evolution of these traits, our sensitivity analyses can be used to make qualitative predictions on how the ECOEVO response and EVO effect might be altered (Fig. 2, Supplementary Fig. 6). For example, strong EVO effects may not be affected if evolving γ_M correlates positively with d_M, whereas weak effects may become strong if γ_M trades-off with d_M. In contrast, the low sensitivity of EVO effects to γ_Z suggests that the evolution of this trait may have little impact on the response of soil C to warming.

The adaptive trait-based approach we use circumvents the difficulty of prescribing critical parameters (such as the enzyme allocation fraction) and their response to environmental change by allowing these parameters to naturally emerge from biologically grounded evolutionary dynamics of the system under study. This approach can easily be extended to predict (rather than assume or prescribe) the adaptive dynamics of multiple microbial traits, such as growth-related traits and substrate-specific enzyme production traits, and their diversification into coexisting functional types. A similar approach has been used to construct a physiology-based model of feedbacks between global ocean ecosystem function and phytoplankton diversity[32]. Rather than assuming values for the multiple physiological traits characterizing each plankton species, that model allowed interactions among randomly parametrized species drive species sorting and emergence of the corresponding trait values. This trait-based approach for microbial communities also facilitates genomic and metagenomic data, mapped to soil microbial function, to be used in model validation [33].

Future extensions of our eco-evolutionary model will enable the mechanistic representation of below-aboveground feedbacks between soil microorganisms and vegetation, by coupling the carbon cycle with other major biogeochemical cycles, such as nitrogen and phosphorus[1]. Existing mathematical[19,34,35] and computational models[20,36,37] pave the way for such extensions. Global projections of the effect of soil microbial evolution on future climate change will become possible (e.g. Wieder et al. 2013) by coupling our eco-evolutionary model of biological decomposition with soil models that account for the chemical and physical transformations of soil carbon occurring on year-to-century timescales[5,38–40].

Given the large population size and short generation time of many microorganisms, biological principles suggest that microbial evolution should be an essential component of ecosystem response to warming. We have shown here that microbial evolutionary adaptation to warming, and its impact on the decomposition of soil organic matter, can radically change soil carbon dynamics. Empirical data suggest that natural values of

enzyme allocation fraction are low[23,34] and fall in the range for which our model predicts large eco-evolutionary responses of decomposition to warming. In spite of an increasing effort to document and understand the ecosystem impact of microbial physiological and ecological responses to climate warming[18,26,41], no Earth system model that seeks to represent the role of living organisms in climate feedbacks has yet included evolutionary mechanisms of adaptation. Our model is a critical first step. We expect projections of future climate and carbon cycle feedbacks, and their uncertainty, to be significantly impacted, from local to global scales.

Methods

We use the microbe-enzyme model of litter decomposition first introduced in ref. 18[18] and extend it to describe the ecological dynamics of soil organic carbon (SOC), dissolved organic carbon (DOC), microbial biomass, and extracellular enzyme abundance, given litter input, leaching rates, and soil temperature (Fig. 1a and Supplementary Fig. 1). The effect of temperature is mediated by enzymes kinetics, with exoenzymes driving the decomposition rate, and intra-cellular enzymes involved in resource uptake and microbial biomass synthesis. As temperature changes, the model predicts how the ecological equilibrium changes. The change in equilibrium SOC is what we call the ecological (ECO) response of the ecosystem.

To investigate the effect of evolutionary adaptation on decomposition, we include microbial evolution in the ecological model. Our focus is on soil bacteria (as opposed to fungi), which typically have large population size and short generation time. We assume that microbes may vary individually in their investment in exoenzymes, measured by the fraction (denoted by φ throughout the paper) of resources allocated to enzyme production. Assuming that some of this variation has a genetic basis, we derive the selection gradient and compute the evolutionarily stable value of the enzyme allocation fraction, φ^*, at any given temperature. We can then evaluate how φ^* changes as temperature increases, and how the ecosystem equilibrium changes from both the direct effect of temperature rise on enzyme kinetics, and the indirect effect mediated by microbial evolutionary adaptation to warming (Fig. 1b, c).

Ecological model. Based on ref. 18[18] (Fig. 1a, Supplementary Fig. 1), the ecological model has four state variables measured in unit mass of carbon: soil (non decomposed) organic carbon (SOC), C; soil decomposed soluble organic carbon (DOC), D; microbial biomass, M; and exoenzyme concentration, Z. Exoenzyme production drives the decomposition process of SOC into DOC, which is the only source of carbon for microbes. The model

accounts for microbial production and death, exoenzyme decay, recycling of dead microbes and degraded exoenzymes, SOC input from plant litter, and leaching of SOC and DOC.

Model equations. State variables C, D, M, Z obey equations (1a-d):

$$\text{(1a)} \quad \frac{dC}{dt} = I - \frac{v_{max}^{D}\, C}{K_m^D + C} Z - e_C C$$

$$\text{(1b)} \quad \frac{dD}{dt} = \frac{v_{max}^{D}\, C}{K_m^D + C} Z + d_M M + d_Z Z - \frac{v_{max}^{U}\, D}{K_m^U + D} M - e_D D$$

$$\text{(1c)} \quad \frac{dM}{dt} = (1 - \varphi)\, \gamma_M \frac{v_{max}^{U}\, D}{K_m^U + D} M - d_M M$$

$$\text{(1d)} \quad \frac{dZ}{dt} = \varphi\, \gamma_Z \frac{v_{max}^{U}\, D}{K_m^U + D} M - d_Z Z$$

In equation (1a), decomposition follows from Michaelis-Menten kinetics of Z binding substrate C; there is a constant input, I, of soil organic (non decomposed) carbon from aboveground litter, and a loss due to leaching at constant rate e_C. In equation (1b), D is produced by decomposition and the recycling of dead microbial biomass and inactive enzymes; D is consumed by microbial uptake, and lost by leaching at constant rate e_D. In equation (1c), growth of microbial biomass M is driven by the rate of DOC uptake (a Monod function of D) times the fraction of uptaken DOC turned into biomass, $(1 - \varphi)\, \gamma_M$, minus microbial mortality at constant rate d_M. In equation (1d), enzyme variation is driven by the rate of DOC uptake times the fraction allocated to enzyme production, φ, and production efficiency, γ_Z, minus enzyme deactivation at constant rate, d_Z.

Ecosystem equilibria. The ecological model possesses either one globally stable equilibrium, or three equilibria (one of which is always unstable) (Supplementary Fig. 2). There are thresholds φ_{min} and φ_{max} such that the globally stable equilibrium exists for $\varphi < \varphi_{min}$ or $\varphi > \varphi_{max}$ and is given by $C = I/e_C$, $D = 0$, $M = 0$, $Z = 0$. Thus, at this equilibrium, the microbial population is extinct and no decomposition occurs. For $\varphi_{min} < \varphi < \varphi_{max}$, the microbial population can either go extinct (then the system stabilizes at the same

equilibrium as before) or persists at or around a non-trivial equilibrium, which can be solved for analytically. Note that $\varphi_{\min}$ and $\varphi_{\max}$ depend on all microbial and model parameters (Supplementary Fig. 3, Supplementary Note 1).

Effect of temperature on model parameters. Decomposition is predicted to respond to warming[5] due to the temperature sensitivity of enzymatic activity[21,22,42]. Microbial assimilation may also vary with temperature if the microbial membrane proteins involved in nutrient uptake are sensitive to warming. Following ref. 18[18], we assume that exoenzyme kinetics parameters (maximum decomposition rate v^D_{max} and half-saturation constant K^D_m) and microbial uptake parameters (maximum uptake rate v^U_{max} and half-saturation constant K^U_m) follow Arrhenius relations with temperature. This defines our baseline 'kinetics-only' scenario of temperature-dependent decomposition:

$$\text{(2a)} \quad v^D_{max} = v^D_0 \, e^{-\frac{E^D_v}{R(T+273)}}$$

$$\text{(2b)} \quad K^D_m = K^D_0 \, e^{-\frac{E^D_K}{R(T+273)}}$$

$$\text{(2c)} \quad v^U_{max} = v^U_0 \, e^{-\frac{E^U_v}{R(T+273)}}$$

$$\text{(2d)} \quad K^U_m = K^U_0 \, e^{-\frac{E^U_K}{R(T+273)}}$$

where T is temperature in Celsius, R is the ideal gas constant, and the E parameters denote the corresponding activation energies.

We consider two additional scenarios for the influence of temperature on decomposition. In the temperature-dependent microbial mortality scenario[25], the microbial death rate increases with temperature. This could be due to a higher risk of predation or pathogenic infection at higher temperatures, or faster microbial senescence due to higher protein turnover[25]. In this scenario, the microbial death rate d_M depends on temperature according to

(3) $$d_M(T) = d_{M0} e^{-\frac{E_{dM}}{R(T+273)}}$$

as in ref. 25[25].

In the temperature-dependent microbial growth efficiency (MGE) scenario, the MGE decreases with temperature[18,25,26], possibly due to higher maintenance costs at higher temperature[27]. This is modeled by making the microbial growth efficiency γ_M vary linearly with temperature[18,22,43,44]:

(4) $$\gamma_M(T) = \gamma_{M,ref} - m\,(T - T_{ref})$$

with T_{ref} = 20 °C.

How scenarios of temperature-dependence and parameter values influence the response of equilibrium C to temperature is shown in Supplementary Fig. 4 and commented on in the Supplementary Note 4.

The enzyme allocation fraction φ is a 'public good' trait: as an individual microbe produces exoenzymes, it experiences an energetic cost and obtains a benefit – access to decomposed organic carbon – that depends on its own and other microbes's production in the spatial neighborhood[45,46]. As a public good trait, φ is under strong direct negative selection: 'cheaters' that produce less or no exoenzymes, and thus avoid the cost while reaping the benefit of enzyme production by cooperative neighbors, should be at a selective advantage. In a highly diffusive environment in which exoenzymes are well mixed, φ would evolve to zero, leading to evolutionary suicide[47]. However, in a more realistic spatially distributed environment with limited exoenzyme diffusion, microbes with a given trait are more likely to interact with phenotypically similar microbes, which puts more cooperative microbes at a competitive advantage over less cooperative strains[45,48,49]. This generates indirect positive selection on trait φ.

The trait value φ^* at which negative and positive selections balance is the evolutionarily stable microbial strategy, given by

$$(5) \qquad \varphi^*(T) = 1 - \frac{d_M}{\gamma_M \, v_{max}^U} - \frac{1}{c_0}$$

where c_0 measures the competitive advantage, due to spatially local interactions, of any given strain over a slightly less cooperative strain, or 'competition asymmetry' (Supplementary Note 3). The parameter c_0 is likely to depend on the diffusivity of DOC, which may itself vary with soil properties such as texture or water content.

As temperature rises from T_0 to T, the direction and magnitude of the microbial adaptive response is measured by $\Delta\varphi^* = \varphi^*(T) - \varphi^*(T_0)$, which depends on the scenario of temperature dependence. The eco-evolutionary (ECOEVO) response of SOC is given by

$$(6) \qquad \text{ECOEVO} = \Delta C_{\text{ECOEVO}}(T_0, T) = C(T, \varphi^*(T)) - C(T_0, \varphi^*(T_0))$$

where $C(T, \varphi)$ denotes ecological equilibrium C at temperature T, given enzyme allocation fraction φ. The ECOEVO response is to be compared with the purely ecological (ECO) response:

$$(7) \qquad \text{ECO} = \Delta C_{\text{ECO}}(T_0, T) = C(T, \varphi^*(T_0)) - C(T_0, \varphi^*(T_0))$$

in which the enzyme allocation fraction is fixed at its T_0-adapted value, $\varphi^*(T_0)$ (Fig. 1c).

We measure the magnitude of the evolutionary (EVO) effect as the difference between the ECOEVO response averaged over the temperature range (T_0, T) and the ECO response averaged over the same temperature range, normalized by the ECO response:

$$(8) \qquad EVO\ effect = \frac{\left| \int_{T_0}^{T} \Delta C_{ECOEVO}(T_0, T) - \int_{T_0}^{T} \Delta C_{ECO}(T_0, T) \right|}{\left| \int_{T_0}^{T} \Delta C_{ECO}(T_0, T) \right|}$$

This evaluation allows us to compare EVO effects across systems that differ in the magnitude of their ECO response. In all simulations we use $T = T_0 + \Delta T$ where $\Delta T = 5$ °C. In general, the ECO and ECOEVO responses are monotonic, close-to-linear functions of T over the considered temperature ranges $(T_0,\ T_0 + \Delta T)$, which makes all our comparative analyses almost insensitive to our choice of ΔT.

Parameters default values and variation range. Under the temperature-dependent kinetics-only scenario, the ecological model (equations (1) and (2)) includes seven microbial parameters (φ, γ_M, d_M, v_0^U, E_v^U, K_0^U, E_K^U), six enzyme parameters (γ_Z, d_Z, v_0^D, E_v^D, K_0^D, E_K^D) and four environmental parameters (I, e_C, e_D, T). Our set of default parameter values is derived from Allison *et al.* (2010) (Supplementary Table 1). The enzyme allocation fraction default value is 10% at 20 °C[34]. For the dependence of enzyme kinetics parameters on temperature, $v_{max}^D(T)$ and $K_m^D(T)$, we selected the Arrhenius equations that best fit data from California[22] (mean annual $T = 17$ °C) and match values at 20 °C (0.42 and 600, respectively)[18]. For the uptake kinetic parameters, we obtained $v_{max}^U(T)$ by selecting v_0^U that best fits the Arrhenius equation in ref. 18[18] with $E_v^U = 35$ and we obtained $K_m^U(T)$ by selecting K_0^U and E_K^U that best fit the linear relation used in ref. 18[18]. To parametrize the temperature-dependent mortality ($d_{M,ref}$, T_{ref}) and MGE ($\gamma_{M,ref}$, m, T_{ref}) models, we used values from ref. 25[25] and tested two values of E_{dM} ($E_{dM} = 0$ is the enzyme only temperature-dependent model). For greater realism, we used a higher value of the exoenzyme deactivation rate (twice the value used in ref. 18[18]) and constrained the range of all parameters in order to enhance stability and produce relative stock sizes that are consistent with empirical data, so that at equilibrium M is about 1% of C, Z is about 1% of M and D is limiting (hence close to 0 at equilibrium[29,30]),

We analysed the model sensitivity by varying parameters over two orders of magnitude (as in ref. 18[18]) – except γ_M and γ_Z for which we used the whole range over which the non-trivial ecosystem equilibrium is stable (Supplementary Table 2). To assess the significance of our findings for real ecosystems, we focused on five biomes for which empirical data[22] could be used to constrain the model. The five biomes contrast strongly in their initial temperature, T_0, and decomposition kinetics, $v_{max}^D(T)$ and $K_m^D(T)$ for which we selected the Arrhenius equations (2) that best fit the relations used in ref. 22[22] (Supplementary Table 3).

References

1. Falkowski, P. G., Fenchel, T. & Delong, E. F. The microbial engines that drive Earth's biogeochemical cycles. *Science* **320**, 1034–1039 (2008).
2. Waksman, S. A. & Starkey, R. L. *The soil and the microbe*. (John Wiley And Sons; New York, 1931).
3. Frey, S. D., Lee, J., Melillo, J. M. & Six, J. The temperature response of soil microbial efficiency and its feedback to climate. *Nat. Clim. Chang.* **3**, 395 (2013).
4. Singh, B. K., Bardgett, R. D., Smith, P. & Reay, D. S. Microorganisms and climate change: terrestrial feedbacks and mitigation options. *Nat. Rev. Microbiol.* **8**, 779–790 (2010).
5. Davidson, E. A. & Janssens, I. A. Temperature sensitivity of soil carbon decomposition and feedbacks to climate change. *Nature* **440**, 165–173 (2006).
6. Bradford, M. A. *et al.* Thermal adaptation of soil microbial respiration to elevated temperature. *Ecol. Lett.* **11**, 1316–1327 (2008).
7. Tucker, C. L., Bell, J., Pendall, E. & Ogle, K. Does declining carbon-use efficiency explain thermal acclimation of soil respiration with warming? *Glob. Chang. Biol.* **19**, 252–263 (2013).
8. Creamer, C. A. *et al.* Microbial community structure mediates response of soil C decomposition to litter addition and warming. *Soil Biol. Biochem.* **80**, 175–188 (2015).
9. Wei, H. *et al.* Thermal acclimation of organic matter decomposition in an artificial

forest soil is related to shifts in microbial community structure. *Soil Biol. Biochem.* **71**, 1–12 (2014).

10. Padfield, D., Yvon-Durocher, G., Buckling, A., Jennings, S. & Yvon-Durocher, G. Rapid evolution of metabolic traits explains thermal adaptation in phytoplankton. *Ecol. Lett.* **19**, 133–142 (2016).
11. Schaum, C.-E. *et al.* Adaptation of phytoplankton to a decade of experimental warming linked to increased photosynthesis. *Nat Ecol Evol* **1**, 94 (2017).
12. Monroe, J. G. *et al.* Ecoevolutionary Dynamics of Carbon Cycling in the Anthropocene. *Trends Ecol. Evol.* **33**, 213–225 (2018).
13. Ratledge, C. Biodegradation of oils, fats and fatty acids. in *Biochemistry of microbial degradation* (ed. Ratledge, C.) 89–141 (Springer Netherlands, 1994).
14. Harder, W. & Dijkhuizen, L. Physiological responses to nutrient limitation. *Annu. Rev. Microbiol.* **37**, 1–23 (1983).
15. Velicer, G. J. Social strife in the microbial world. *Trends Microbiol.* **11**, 330–337 (2003).
16. Trivedi, P. *et al.* Microbial regulation of the soil carbon cycle: evidence from gene-enzyme relationships. *ISME J.* **10**, 2593–2604 (2016).
17. Rainey, P. B. & Rainey, K. Evolution of cooperation and conflict in experimental bacterial populations. *Nature* **425**, 72–74 (2003).
18. Allison, S. D., Wallenstein, M. D. & Bradford, M. A. Soil-carbon response to warming dependent on microbial physiology. *Nat. Geosci.* **3**, 336 (2010).

19. Sinsabaugh, R. L. & Moorhead, D. L. Resource allocation to extracellular enzyme production: A model for nitrogen and phosphorus control of litter decomposition. *Soil Biol. Biochem.* **26**, 1305–1311 (1994).

20. Allison, S. D. A trait-based approach for modelling microbial litter decomposition. *Ecol. Lett.* **15**, 1058–1070 (2012).

21. Wallenstein, M. D., Mcmahon, S. K. & Schimel, J. P. Seasonal variation in enzyme activities and temperature sensitivities in Arctic tundra soils. *Glob. Chang. Biol.* **15**, 1631–1639 (2009).

22. German, D. P., Marcelo, K. R. B., Stone, M. M. & Allison, S. D. The Michaelis-Menten kinetics of soil extracellular enzymes in response to temperature: a cross-latitudinal study. *Glob. Chang. Biol.* **18**, 1468–1479 (2012).

23. Burns, R. G. *et al.* Soil enzymes in a changing environment: Current knowledge and future directions. *Soil Biol. Biochem.* **58**, 216–234 (2013).

24. Hochachka, P. W. & Somero, G. N. *Biochemical Adaptation: Mechanism and Process in Physiological Evolution*. (Oxford University Press, 2002).

25. Hagerty, S. B. *et al.* Accelerated microbial turnover but constant growth efficiency with warming in soil. *Nat. Clim. Chang.* **4**, 903 (2014).

26. Wieder, W. R., Bonan, G. B. & Allison, S. D. Global soil carbon projections are improved by modelling microbial processes. *Nat. Clim. Chang.* **3**, 909 (2013).

27. Sinsabaugh, R. L., Manzoni, S., Moorhead, D. L. & Richter, A. Carbon use efficiency of microbial communities: stoichiometry, methodology and modelling. *Ecol. Lett.* **16**,

930–939 (2013).

28. Conant, R. T. *et al.* Temperature and soil organic matter decomposition rates - synthesis of current knowledge and a way forward. *Glob. Chang. Biol.* **17**, 3392–3404 (2011).

29. Fierer, N., Strickland, M. S., Liptzin, D., Bradford, M. A. & Cleveland, C. C. Global patterns in belowground communities. *Ecol. Lett.* **12**, 1238–1249 (2009).

30. Ladd, J. N., Amato, M., Zhou, L.-K. & Schultz, J. E. Differential effects of rotation, plant residue and nitrogen fertilizer on microbial biomass and organic matter in an Australian alfisol. *Soil Biol. Biochem.* **26**, 821–831 (1994).

31. Wallenstein, M. D. & Hall, E. K. A trait-based framework for predicting when and where microbial adaptation to climate change will affect ecosystem functioning. *Biogeochemistry* **109**, 35–47 (2012).

32. Follows, M. J., Dutkiewicz, S., Grant, S. & Chisholm, S. W. Emergent biogeography of microbial communities in a model ocean. *Science* **315**, 1843–1846 (2007).

33. Trivedi, P., Anderson, I. C. & Singh, B. K. Microbial modulators of soil carbon storage: integrating genomic and metabolic knowledge for global prediction. *Trends Microbiol.* **21**, 641–651 (2013).

34. Schimel, J. P. & Weintraub, M. N. The implications of exoenzyme activity on microbial carbon and nitrogen limitation in soil: a theoretical model. *Soil Biol. Biochem.* **35**, 549–563 (2003).

35. Harte, J. & Kinzig, A. P. Mutualism and competition between plants and

decomposers: implications for nutrient allocation in ecosystems. *Am. Nat.* **141**, 829–846 (1993).

36. Kaiser, C., Franklin, O., Dieckmann, U. & Richter, A. Microbial community dynamics alleviate stoichiometric constraints during litter decay. *Ecol. Lett.* **17**, 680–690 (2014).
37. Kaiser, C., Franklin, O., Richter, A. & Dieckmann, U. Social dynamics within decomposer communities lead to nitrogen retention and organic matter build-up in soils. *Nat. Commun.* **6**, 8960 (2015).
38. Abramoff, R. *et al.* The Millennial model: in search of measurable pools and transformations for modeling soil carbon in the new century. *Biogeochemistry* **137**, 51–71 (2018).
39. Bradford, M. A. *et al.* Managing uncertainty in soil carbon feedbacks to climate change. *Nat. Clim. Chang.* **6**, 751 (2016).
40. Schmidt, M. W. I. *et al.* Persistence of soil organic matter as an ecosystem property. *Nature* **478**, 49–56 (2011).
41. Treseder, K. K. *et al.* Integrating microbial ecology into ecosystem models: challenges and priorities. *Biogeochemistry* **109**, 7–18 (2012).
42. Stone, M. M. *et al.* Temperature sensitivity of soil enzyme kinetics under N-fertilization in two temperate forests. *Glob. Chang. Biol.* **18**, 1173–1184 (2012).
43. Wang, G., Post, W. M. & Mayes, M. A. Development of microbial-enzyme-mediated decomposition model parameters through steady-state and dynamic analyses. *Ecol. Appl.* **23**, 255–272 (2013).

44. Li, J., Wang, G., Allison, S. D., Mayes, M. A. & Luo, Y. Soil carbon sensitivity to temperature and carbon use efficiency compared across microbial-ecosystem models of varying complexity. *Biogeochemistry* **119**, 67–84 (2014).

45. Allison, S. D. Cheaters, diffusion and nutrients constrain decomposition by microbial enzymes in spatially structured environments: Constraints on enzymatic decomposition. *Ecol. Lett.* **8**, 626–635 (2005).

46. Nadell, C. D., Drescher, K. & Foster, K. R. Spatial structure, cooperation and competition in biofilms. *Nat. Rev. Microbiol.* **14**, 589–600 (2016).

47. Ferriere, R. & Legendre, S. Eco-evolutionary feedbacks, adaptive dynamics and evolutionary rescue theory. *Philos. Trans. R. Soc. Lond. B Biol. Sci.* **368**, 20120081 (2013).

48. Durrett, R. & Levin, S. The Importance of Being Discrete (and Spatial). *Theor. Popul. Biol.* **46**, 363–394 (1994).

49. Chao, L. & Levin, B. R. Structured habitats and the evolution of anticompetitor toxins in bacteria. *Proc. Natl. Acad. Sci. U. S. A.* **78**, 6324–6328 (1981).

End Notes

Acknowledgements We thank Rachel Gallery, Pierre-Henri Gouyon, Moira Hough, Hélène Leman, Laura Meredith, and Mitch Pavao-Zuckerman for discussion. E.A. was supported by fellowships from Ecole Doctorale Frontières du Vivant and MemoLife Laboratory of Excellence (PIA-10-LBX-54). S.R.S. was supported by a grant from the Genomic Science Program of the United States Department of Energy (DOE) (DE-SC0016440) and the University of Arizona's Agnese Nelms Haury Program in Environment and Social Justice. R.F. acknowledges support from FACE Partner University Fund, CNRS Mission pour l'Interdisciplinarité, and PSL University (IRIS OCAV and PSL-University of Arizona Mobility Program).

Author contributions R.F. conceived the study. All authors developed the model. E.A. performed the analysis. E.A. and R.F. wrote the first version of the manuscript. All authors finalized the paper.

Competing interests The authors declare no competing interests.

Additional information

Supplementary information is available for this paper at https://doi.org/xxx

Correspondence and requests for materials should be addressed to E.A. or R.F.

Figure Captions

Figure 1. Effect of temperature and enzyme allocation fraction on SOC ecological equilibrium. **a**, Structure of the microbial-enzyme ecological model (see Methods for details): SOC stock is the balance of plant input, I, loss from leaching, lc, and loss by exoenzyme-mediated degradation to DOC (D), which in turn is allocated between (fraction φ) production of enzymes (Z) and (fraction $1-\varphi$) growth of microbial biomass (M). **b**, Effect of temperature, T, and enzyme allocation fraction, φ, on SOC equilibrium, C, in the baseline scenario of temperature dependence. **c**, Response of SOC ecological equilibrium, C, to a 5°C increase in temperature (from 20 °C to 25 °C) as a function of enzyme allocation fraction, φ. Parameters are set to their default values (Supplementary Table 1), except $I = 5\ 10^{-3}$, $v_0^U = 10^5$, $E_v^U = 38$ and $c_0 = 1.17$.

gFigure 2. Effect of microbial evolutionary adaptation on the SOC equilibrium response to + 5 °C warming (EVO effect). Temperature influences enzyme kinetics only (baseline scenario of temperature dependence). **a**, Influence of microbial biomass production efficiency, γ_M, and microbial mortality rate, d_M. **b**, Influence of microbial resource acquisition traits v_0^U and E_v^U. **c-d**, Influence of competition asymmetry, c_0, and initial temperature, T_0. In all figures, constant parameters are set to their default values (Supplementary Table 1) and I is set to $5\ 10^{-3}$. Points A1 and B1 indicate the default parameter values. Point A2 (respectively B2) exemplifies values of γ_M and d_M (resp. v_0^U and E_v^U) for which the EVO effect is strong. Panel **c** (resp. **d**) shows the influence of c_0 and T_0 on the EVO effect at A2 (resp. B2).

Figure 3. Ecological and eco-evolutionary responses of SOC equilibrium to warming (up to + 5 °C) for three scenarios of temperature dependence. Ecological and eco-evolutionary changes in SOC equilibrium C given by Eq. (3a) (without evolution, dashed curves) and Eq. (3b) (with evolution, plain curves) are plotted as a function of the increase in temperature. *Blue curves*, initial temperature T_0 = 5°C. *Black curves*, $T_0 = T_{ref}$ = 20°C. *Red curves*, T_0 = 30°C. *Insets*, Direction and magnitude of EVO effect (%), from - 150 % to + 150 %, color code indicates T_0 as before. **a**, Baseline scenario of temperature dependence (enzyme kinetics only). **b**, Temperature-dependent microbial turnover, with $E_{dM} = 25 < E_v^U$. **c**, Temperature- dependent microbial turnover, with $E_{dM} = 55 > E_v^U$. **d**, Temperature-dependent MGE, with m = - 0.014. Parameters values correspond to point B2 in Fig. 2 ($I = 5\ 10^{-3}$, $v_0^U = 10^5$, $E_v^U = 38$, $c_0 = 1.17$); other parameters are set to their default values (Table S1).

Figure 4. Ecological and eco-evolutionary responses of SOC equilibrium to + 5 °C warming predicted for five biomes. a-d, ECO response. **e-h**, ECOEVO response. **i-l,** EVO effect. AK: Alaska, boreal forest, T_0 = 0.1°C. ME: Maine, temperate forest, T_0 = 5°C. WV: West Virginia, temperate forest, T_0 = 9°C. CA: California, temperate grassland, T_0 = 17°C. CR: Costa Rica, tropical rain forest, T_0 = 26°C. First column (**a, e, i**): baseline scenario of temperature dependence. Second column (**b, f, j**): temperature-dependent microbial turnover scenario with $E_{dM} = 25 < E_v^U$. Third column (*c*, *g*, *k*): temperature-dependent microbial turnover scenario with $E_{dM} = 55 > E_v^U$. Fourth column (**d, h, l**): temperature-dependent MGE scenario (m = - 0.014). The influence of competition asymmetry, c_0, is shown. For clarity, vertical axis for ECO and ECOEVO responses are truncated at - 65 mg C cm^{-3}. Actual values for AK with c_0 = 1.17 are ECO = - 170 mg C cm^{-3} and ECOEVO = - 556 mg C cm^{-3} ; actual value for WV with c_0 = 1.17 is ECOEVO = - 92.8 mg C cm^{-3}. Parameters values correspond to point B2 in Fig. 2 ($I = 5\ 10^{-3}$, $v_0^U = 10^5$,

$E_v^U = 38$, $c_0 = 1.17$); other parameters are set to their default values (Supplementary Table 1).

Figure 1

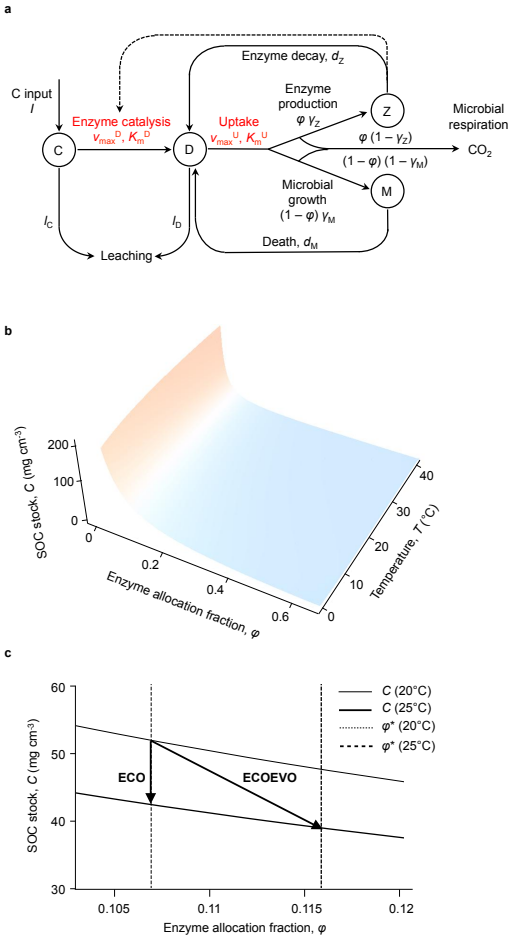
a
C input
I
Enzyme catalysis
v_{max}^{D}, K_m^{D}
Enzyme decay, d_Z
Enzyme
production
$\varphi\,\gamma_Z$
Uptake
v_{max}^{U}, K_m^{U}
Z
Microbial
respiration
C
D
$\varphi\,(1-\gamma_Z)$
$(1-\varphi)\,(1-\gamma_M)$
CO_2
Microbial
growth
$(1-\varphi)\,\gamma_M$
M
I_C
I_D
Leaching
Death, d_M
b
SOC stock, C (mg cm^{-3})
200
100
0
0
0.2
0.4
0.6
Enzyme allocation fraction, φ
0
10
20
30
40
Temperature, T (°C)
c
60
50
40
30
SOC stock, C (mg cm^{-3})
ECO
ECOEVO
0.105
0.11
0.115
0.12
Enzyme allocation fraction, φ
C (20°C)
C (25°C)
φ* (20°C)
φ* (25°C)

Figure 2

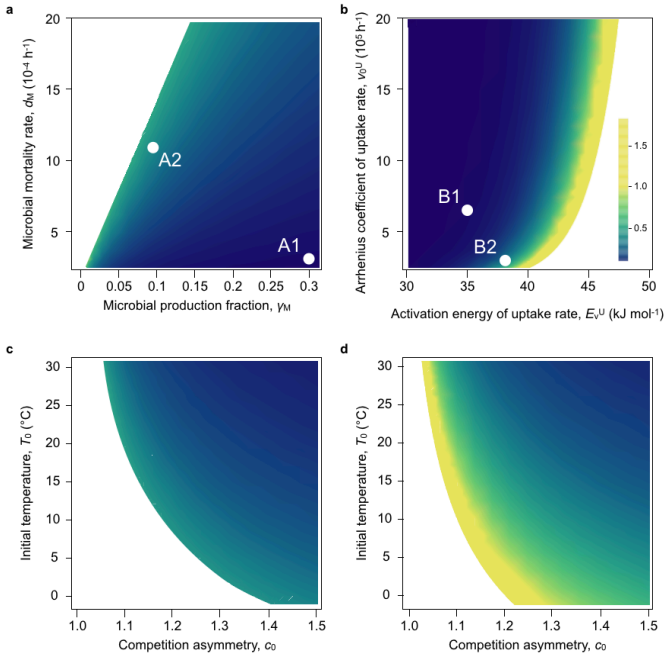
a
b
c
d
Microbial mortality rate, d_M (10^{-4} h^{-1})
Microbial production fraction, γ_M
A1
A2
Arrhenius coefficient of uptake rate, v_0^U (10^5 h^{-1})
Activation energy of uptake rate, E_v^U (kJ mol^{-1})
B1
B2
Initial temperature, T_0 (°C)
Competition asymmetry, c_0

Figure 3

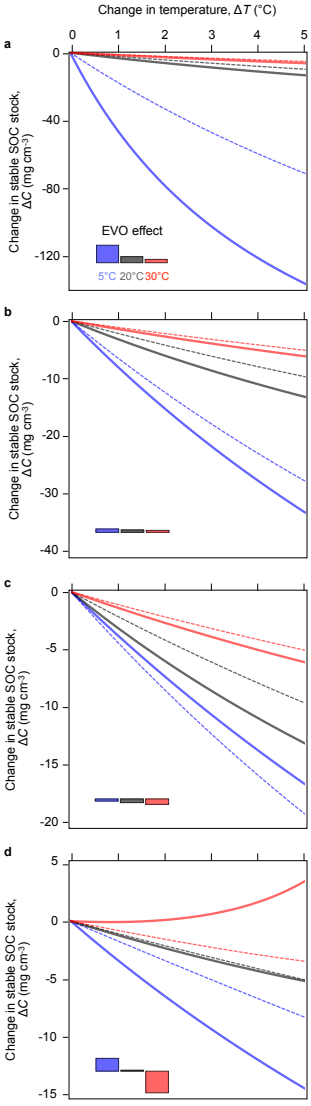
Change in temperature, ΔT (°C)
a
b
c
d
Change in stable SOC stock, ΔC (mg cm⁻³)
EVO effect
5°C 20°C 30°C

Figure 4

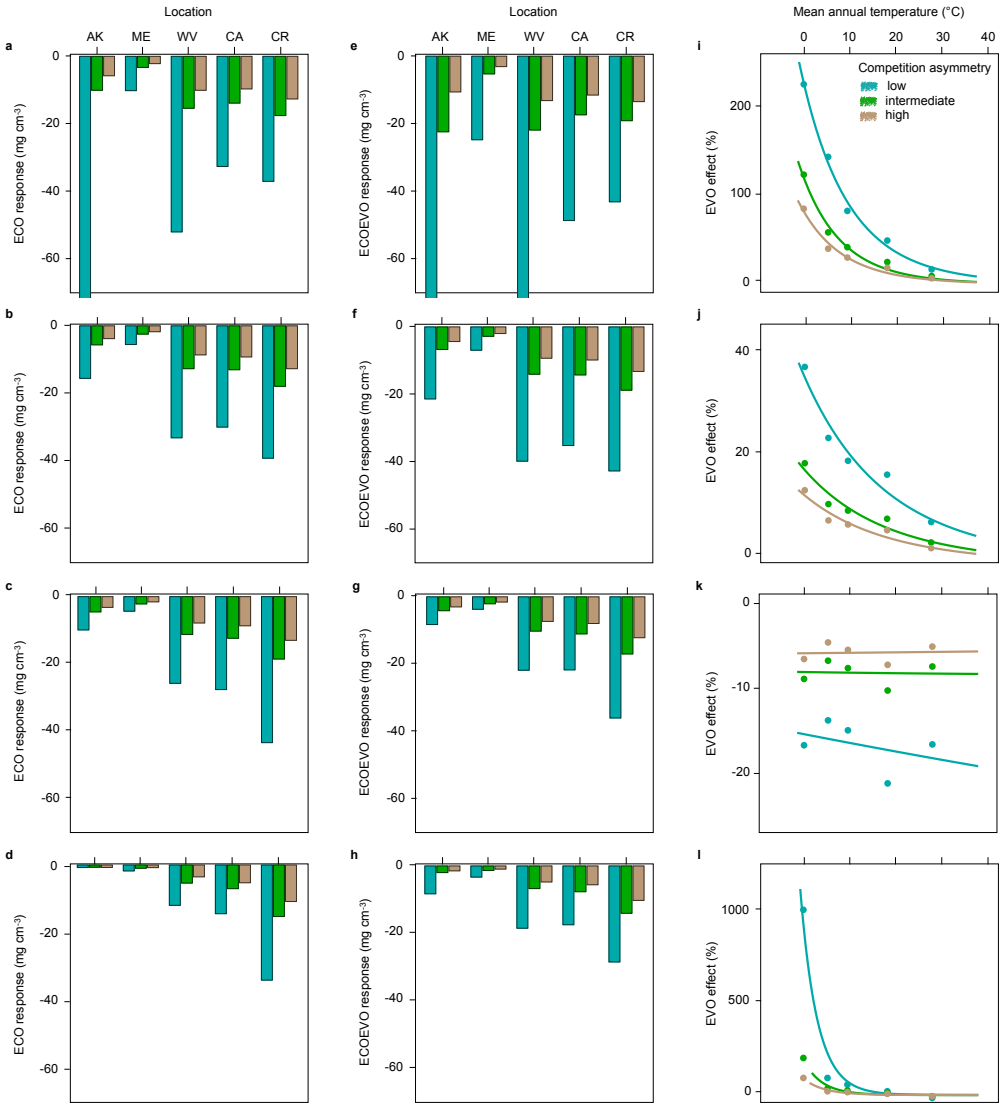
Location
AK
ME
WV
CA
CR
Mean annual temperature (°C)
0
10
20
30
40
Competition asymmetry
low
intermediate
high
a
b
c
d
e
f
g
h
i
j
k
l
ECO response (mg cm⁻³)
ECOEVO response (mg cm⁻³)
EVO effect (%)
0
-20
-40
-60
200
100
40
20
-10
1000
500